THE PROBABLE DETECTION OF SN 1923A: THE OLDEST RADIO SUPERNOVA?

Christopher R. Eck[1], Douglas A. Roberts[2], John J. Cowan[1] and David Branch[1]

eck@mail.nhn.ou.edu, dougr@ncsa.uiuc.edu, cowan@mail.nhn.ou.edu, branch@mail.nhn.ou.edu

Received ____________; accepted ____________

[1]Department of Physics and Astronomy, University of Oklahoma, Norman, OK 73019

[2]Department of Astronomy, University of Illinois, Urbana, IL 61801

ABSTRACT

Based upon the results of VLA observations, we report the detection of two unresolved radio sources that are coincident with the reported optical position of SN 1923A in M83. For the source closest to the SN position, the flux density was determined to be 0.30 ± 0.05 mJy at 20 cm and 0.093 ± 0.028 mJy at 6 cm. The flux density of the second nearby source was determined to be 0.29 ± 0.05 at 20 cm and 0.13 ± 0.028 at 6 cm. Both sources are non-thermal with spectral indices of $\alpha = -1.0 \pm 0.30$ and -0.69 ± 0.24, respectively. SN 1923A has been designated as a Type II-P. No Type II-P (other than SN 1987A) has been detected previously in the radio. The radio emission from both sources appears to be fading with time. At an age of approximately 68 years when we observed it, this would be the oldest radio supernova (of known age) yet detected.

Subject headings: circumstellar matter — supernovae: general — supernovae: individual (SN 1923A) — galaxies : individual (NGC 5236)

1. Introduction

Some Type II supernovae have exhibited radio emission within a few years of explosion, including SNe 1970G in M101 (Gottesman et al. 1972; Allen et al. 1976), 1978K in NGC 1313 (Ryder et al. 1993), 1979C in M100 (Weiler et al. 1986), 1980K in NGC 6946 (Weiler et al. 1986, 1992), 1981K (van der Hulst et al. 1983; Weiler et al. 1986), 1986J in NGC 891 (Rupen et al. 1987), 1988Z in MCG +03-28-022 (Van Dyk et al. 1993b) and 1993J in NGC 3031 (Van Dyk et al. 1994). In addition SN 1987A was detected in the radio shortly after outburst (see Turtle et al. 1987), but at a level significantly below that seen from the more distant Type II supernovae and from the Galactic SNR Cas A. Radio emission was also detected for a brief period from two Type Ibs, 1983N and 1984L (Sramek, Panagia, & Weiler 1984; Weiler et al. 1986; Weiler & Sramek 1988), and from the Type Ic supernova 1990B (Van Dyk et al. 1993a). No Type Ia SNe have been detected in the radio despite several searches (e.g. Eck et al. 1995).

Radio emission from supernova remnants (SNRs) is typically observed long after the supernova phase. Such factors as the density of the local interstellar medium affect the turn-on time in models such as those of Cowsik & Sarkar (1984) based upon the Gull (1973) piston model. These models typically suggest a minimum of 100 years for the formation and brightening of an SNR. SN 1987A is already indicating an increase in brightness with time (Gaensler et al. 1997), but it is entering a phase of delayed circumstellar interaction.

We (Cowan & Branch 1982, 1985) have defined intermediate-age supernovae, from $\sim$ 10–300 years old, as spanning the period well after the optical emission fades (typically about 2 years) and before the turn-on of radio emission from an SNR (assumed to take at least 100 years). This time period is critical in understanding the later stages of stellar evolution. In particular, the circumstellar mass loss rate for the supernova progenitors is a critical component in the initiation and duration of radio emission in the models of

Chevalier (1982, 1984).

To study this transition period, we and others have attempted to detect radio emission from intermediate-age supernovae. While there have been a number of unsuccessful searches (see Eck et al. 1995, Eck et al. 1996, Eck, Cowan, & Branch 1998), SNe 1950B & 1957D in M83 (Cowan & Branch 1985, Cowan, Roberts, & Branch 1994 = CRB), SN 1968D in NGC 6946 (Hyman et al. 1995) and SN 1970G in M101 (Cowan, Goss, & Sramek 1991) have been detected in the radio more than a decade after explosion. (SN 1961V was also detected [Branch & Cowan 1985, Cowan, Henry, & Branch 1988], but there is uncertainty about whether it really was a supernova [Filippenko et al. 1995].) We also note that while the radio emission from SN 1980K has abruptly dropped after approximately ten years (Weiler et al. 1992, Montes et al. 1998), SN 1979C (at a greater distance than SN 1980K) is still emitting at detectable levels (Weiler et al. 1991)

In this *Letter* we report the probable detection of SN 1923A in M83, which at an age of $\sim$ 68 years would be the oldest intermediate-age supernova of known age.

2. Observations and Data Reduction

SN 1923A was discovered by C. Lampland (Lampland 1936) in M83, classified as an SABc starburst galaxy at 4.1 Mpc (Saha et al. 1996) and home to 5 other supernovae (SNe 1945B, 1950B, 1957D, 1968L, 1983N). Its position via offsets to the center of M83 is $109''$ E and $58''$ N. A recent re-analysis of the map of M83 from CRB revealed two faint sources near the optical position of SN 1923A.

Observations of M83 were made at two epochs for each wavelength, 20 and 6 cm, at the Very Large Array (VLA)[3] in different configurations such that the beam sizes were circular

[3]The VLA is a telescope of the National Radio Astronomy Observatory which is operated

and approximately the same for all observations. The different "hybrid" configurations were used at the VLA to obtain circular beam sizes for observations of M83, at low declination. The phase and pointing centers for all images were at R.A.(1950)= $13^{h}34^{m}12\overset{s}{.}2$, Dec.(1950)= $-29^{\circ}35'36\overset{\prime\prime}{.}0$ and the strong radio source 3C 286 was used as primary flux calibrator for all observations.

Due to the non-thermal nature of the late-time radio emission from supernovae, M83 was observed initially at 20 cm at the first epoch, and then at 6 cm to determine the spectral index of the observed sources. At the second epoch a problem with the online systems at the VLA corrupted the 20 cm data taken in the hybrid BnA configuration. The observations were repeated later in B configuration instead, resulting in a slightly different beam size than at the first epoch at 20 cm. Table 1 summarizes the relevant parameters for each wavelength and epoch.

The data reduction was done using the Astronomical Image Processing System (AIPS) software provided by the National Radio Astronomy Observatory. Details of the original data reduction techniques are described in the papers regarding the observations of M83 (Cowan & Branch 1985, CRB). While a Maximum Entropy Method was used in the original image processing to reconstruct the diffuse structure, we have used CLEAN for the second epoch observations to get a higher signal-to-noise for isolated point sources (i.e., SN 1923A) where the diffuse structure was not important. We initially attempted to fit the two nearby point sources with two Gaussian components simultaneously using JMFIT, however, the relatively low signal-to-noise ratio of the two sources prevented convergence. Therefore, all but one of the flux densities and positions were determined by fitting a quadratic function to each source, using the MAXFIT program of the AIPS package. For the other

---

by Associated Universities, Inc., under a cooperative agreement with the National Science Foundation.

datum, the fit using MAXFIT failed so that we report the peak flux using the AIPS routine IMSTAT. A background level was estimated using TVSTAT at all wavelengths and epochs. The background level was determined to be on the order of the rms noise so it was included in the error estimation. PBCOR was used to correct the fluxes for primary beam attenuation. Images of the field of view can be seen in Figure 1 and results for positions and fluxes are given in Table 2, along with the optical supernova position from Pennington, Talbot, & Dufour (1982). Figure 1a shows approximately half of M83 at 20 cm along with several sources CRB observed, labeled here as in that paper. Figure 1b shows the region surrounding SN 1923A (zoomed in from Figure 1a) and includes both SN candidates. Figure 1c is a 6cm map of approximately the same region as in Figure 1b. To within the uncertainties[4], both unresolved sources are coincident with the optical position. Although we tentatively report the western (closer) source as probably being from SN 1923A, we cannot exclude the possibility that either source may be SN 1923A. Calculation of the spectral index, α, ($S \propto \nu^{\alpha}$) between 20 and 6 cm (at second epoch only) reveals that both candidates are non-thermal, with the western source at $\alpha_6^{20} = -1.0 \pm 0.30$ and the eastern source at $\alpha_6^{20} = -0.69 \pm 0.24$. Some caution must be exercised in interpreting this value since the flux densities were measured at slightly different times. We can compare this value to the late-time spectral indices of other Type II SNe ($\alpha_6^{20} = -0.57$ [1950B, CRB], -0.23 1957D, CRB][5], -0.60 [1961V, Cowan et al. 1988], -0.92 [1968D, Hyman et al. 1995], -0.59 [1970G, Cowan et al. 1991], -0.74 [1979C, Weiler et al. 1991]).

[4]Without a fitting routine such as JMFIT to estimate positional uncertainty, we can only report the beamsize as representative of the positional uncertainty although it is probably less than this.

[5]Note: this value is at the first epoch of observations since it is believed the SN has faded below the level of an associated H II region at the second epoch (CRB)

Since there are 6 cm flux densities at two epochs, it is tempting to try to fit the data to a power-law in time ($S \propto t^{\beta}$) for comparison with other events ($\beta_{20\mathrm{cm}} = -2.9, \beta_{6\mathrm{cm}} = -1.7$[1957D,CRB], $\beta_{20\mathrm{cm}} = -1.95$[1970G,Cowan, Goss, & Sramek 1991]). For SN 1923A we find $\beta_{6\mathrm{cm}} = -6.9 \pm 4.0$ and -4.7 ± 3.3 for the western and eastern sources, respectively. Since the flux densities appear to be decreasing with time, both sources are consistent with being in the later stages of radio supernova evolution. While it is likely that both sources are fading radio SNe, it is not clear which source is SN 1923A.

3. Discussion and Conclusions

Although the detected sources are relatively weak, the non-thermal nature and the apparent positional coincidence with the location of SN 1923A (as shown in Table 2) make it probable that we have detected radio emission from this supernova. The sources are separated by about $3\overset{''}{.}5$ which, at the distance to M83 (4.1 Mpc), corresponds to almost 70 pc, thus the sources cannot both be from SN 1923A. Past optical studies of the site of SN 1923A have shown evidence for an H II region at or near the supernova site. Rumstay & Kaufman (1983) list an H II region — no. 59 in their paper — within $1'' - 2''$ of the SN position as based upon offsets with respect to the center of its parent galaxy. Richter & Rosa (1984) refer to Rumstay & Kaufman H II region no. 59 as an H II region associated with and lying $1''$ from SN 1923A. Pennington et al. (1982) also note that SN 1923A appears to be coincident with an H II region. A map of H II regions by de Vaucouleurs, Pence, & Davoust (1983), when overlaid with the scaled radio map, has our source for SN 1923A directly over the H II region. Since the progenitor star of SN 1923A has been estimated to have been massive, $\simeq 18$ $M_{\odot}$ (Pennington et al. 1982), it should not have moved much prior to explosion, and the H II region near the radio source may be associated with the supernova's progenitor. The presence of an H II region at the SN site reduces the chances that the two sources are actually background sources. There is evidence for other similar associations of radio supernovae (RSNe) and H II regions (Van Dyk 1992), including SN 1957D (also estimated to have resulted from a massive star) in M83 (CRB). Clearly new examinations of the area surrounding the site of SN 1923A in M83 to search for an optical counterpart to the radio source are warranted.

On the basis of what is known about the shape of its light curve, SN 1923A has been tentatively designated as a sub-luminous Type II-P (Patat et al. 1994, Schaefer 1996). No Type II-P (other than SN 1987A) has been detected previously in the radio. In Figure 2, we plot the radio luminosity at 20 cm of the new source assuming it to be SN 1923A, along with several other extra-galactic RSNe and two Galactic SNRs, as a function of time since outburst. Data and fits (solid lines) in Figure 2 for the well-studied Type II-L SN 1979C were taken from Weiler et al. (1986, 1991), for the Type II-L SN 1980K from Weiler et al. (1986, 1992), for the Type Ib SN 1983N from Weiler et al. (1986) and Cowan & Branch (1985), for the Type II-L SN 1970G from Cowan et al. (1991), for the Type II-L SN 1968D from Hyman et al. (1995) and for SNe 1950B & 1957D from CRB. The distance to M83 (4.1 Mpc) was taken to be the Cepheid–based distance to NGC 5253, (Saha et al. 1995), a fellow member of the Centaurus group. As Figure 2 illustrates, the luminosity of SN 1923A is comparable to, but slightly below, the two other intermediate-age supernovae we have detected in M83, SNe 1957D and 1950B. (These two supernovae are suspected to have had massive progenitors but their actual supernova types are unknown.) SN 1957D may actually be somewhat less luminous than plotted, because emission from an associated H II region may have contributed to the observed flux. The radio emission from SN 1923A falls between that of Cas A and the Crab.

At an age of approximately 68 years when last observed, SN 1923A would be the oldest radio supernova yet discovered. Detectable radio emission from supernovae decades after explosion (but before the SNR phase) may in fact be uncommon, as evidenced by the small class of such known objects. Observations of several other supernovae over a number of years also support that conclusion. While SN 1979C is still detectable, SN 1980K has dropped off sharply after a decade of being followed. Recently Montes et al. (1997) have reported early-time radio emission from SN 1986E, while we were unable to detect this supernova at an intermediate-age despite a deep VLA search (Eck et al. 1996). Montes et al. (1997) argue that SN 1986E is a typical Type II-L, similar to SN 1980K and the fading radio emission can be adequately explained in terms of the Chevalier model.

What is the cause of the radio emission of SN 1923A? No Type II-P events have been observed to undergo a prompt, bright circumstellar interaction such as that of radio supernovae. SN 1987A, having been a sub-luminous Type II-P, underwent a prompt but dim circumstellar interaction that would not have been detectable in a galaxy beyond the local group, but now it is beginning what promises to be stronger, delayed interaction with a detached circumstellar shell that originated back in its red giant days. If SN 1923A was a sub-luminous Type II–P, it may now be fading from the kind of delayed interaction that SN 1987A is just beginning.

The key radio observations needed now (apart from more firmly establishing the presence of a non-thermal radio source at the site of SN 1923A) are to trace the radio evolution of these sources, one of which is likely to be SN 1923A, the oldest radio supernova yet detected. While we noted above that theoretical models have suggested a minimum time of 100 years for the onset of the SNR (and a brightening) phase, radio emission from the supernovae at this age has never been previously detected or studied. Our observations at one wavelength seem to indicate that the source closest to the SN position is still fading with time, but our uncertainties are large. Additional observations of SN 1923A will help to understand more about the nature of radio emission as supernovae evolve from intermediate-age to the SNR phase.

We wish to thank the anonymous referee for invaluable comments and suggestions to improve our paper. This work has been supported in part by NSF grants AST-9314936, AST-9618332 and AST-9417102 at the University of Oklahoma. This paper was begun when J.J.C. was in residence at the Institute for Theoretical Physics at the University of California Santa Barbara and supported in part by the National Science Foundation under Grant No. PHY94-07194.

REFERENCES

Allen, R. J., Goss, W. M., Ekers, R. D., & de Bruyn, A. G. 1976, A&A, 48, 253

Branch, D., & Cowan, J. J. 1985, ApJ, 297, L33

Chevalier, R. A. 1982, ApJ, 259, 302

—–. 1984, ApJ, 285, L63

Cowan, J. J., & Branch, D. 1982, ApJ, 258, 31

Cowan, J. J., & Branch, D. 1985, ApJ, 293, 400

Cowan, J. J., Henry, R. B. C., & Branch. D. 1988, ApJ, 329, 116

Cowan J. J., Goss, W. M., & Sramek, R. A. 1991, ApJ, 379, L49

Cowan, J. J., Roberts, D. A., & Branch, D. 1994, ApJ, 434, 128

Cowsik, R., & Sarkar, S. 1984, MNRAS, 207, 745

de Vaucouleurs, D. G., Pence, W. D., & Davoust, E. 1983, ApJS, 53, 17

Eck, C. R., Cowan, J. J., Roberts, D., Boffi, F. R., & Branch, D. 1995, ApJ, 451, L53

Eck, C. R., Cowan, J. J., Boffi, F. R., & Branch, D. 1996, ApJ, 472, L25

Eck, C. R., Cowan, J. J., & Branch, D. 1998, in preparation

Filippenko, A. V., Barth, A. J., Bower, G. C., Ho, L. C., Stringfellow, G. S., Goodrich, R. W., & Porter, A. C. 1995, AJ, 110, 2261

Gaensler, B. M., Manchester, R. N., Staveley-Smith, L., Tzioumis, A. K., Reynolds, J. E., & Kesteven, M. J. 1997, ApJ, 479, 845

Gottesman, S. T., Broderick, J. J., Brown, R. L., Balick, B., & Palmer, P. 1972, ApJ, 174, 383

Gull, S. F. 1973, MNRAS, 161, 47

Hyman, S. D., Van Dyk, S. D., Weiler, K. W., & Sramek, R. A. 1995, ApJ, 443, L77

Lampland, C. O., 1936, PASP, 48, 320

Montes, M. J., Van Dyk, S. D., Weiler, K. W., Sramek, R. A., & Panagia, N. 1997, ApJ, 482, L61

Montes, M. J., Van Dyk, S. D., Weiler, K. W., Sramek, R. A., & Panagia, N. 1998, ApJ, in press.

Patat, F., Barbon, R., Cappellaro, E., & Turatto, M. 1994, A&A, 282, 731

Pennington, R. L., Talbot, R. J., & Dufour, R. 1982, AJ, 87, 1538

Richter, O.-G., & Rosa, M. 1984, A&A, 140, L1

Rumstay, K. S., & Kaufman, M. 1983, ApJ, 274, 611

Rupen, M. P., van Gorkom, J. H., Knapp, G. R., Gunn, J. E., & Schneider, D. P. 1987, AJ, 94, 61

Ryder, S., Stavely-Smith, L., Dopita, M., Petre, R., Colbert, E., Malin, D., & Schlegel, E. 1993, ApJ, 416, 167

Saha, A., Sandage, A., Labhardt, L., Schwengler, H., & Machetto, F. D. 1995, ApJ, 438, 8

Schaefer, B. E. 1996, ApJ, 464, 404

Sramek, R. A., Panagia, N., & Weiler, K. W. 1984, ApJ, 285, L59

Turtle, A. J., Campbell-Wilson, D., Bunton, J. D., Jauncey, D. L., Kesteven, M. J., Manchester, R. N., Norris, R. P., Storey, M. C., & Reynolds, J. E. 1987, Nature, 327, 38

van der Hulst, J. M., Hummel, F., Davies, R. D., Pedlar, A., & van Albada, G. D. 1983, Nature, 306, 566

Van Dyk, S. D., AJ, 103, 1788

Van Dyk, S. D., Sramek, R. A., Weiler, K. W., & Panagia, N. 1993a, ApJ, 409, 162

Van Dyk, S. D., Weiler, K. W., Sramek, R. A., & Panagia, N., 1993b, ApJ, 419, L69

Van Dyk, S. D., Weiler, K. W., Sramek, R. A., Rupen, M., & Panagia, N., 1994, ApJ, 432, L115

Weiler, K. W., & Sramek, R. A. 1988, ARA&A, 26, 295

Weiler, K. W., Sramek, R. A., Panagia, N., van der Hulst, J. M., & Salvati, M. 1986, ApJ, 301, 790

Weiler, K. W., Van Dyk, S. D., Panagia, N., & Sramek, R. A. 1992, ApJ, 398, 248

Weiler, K. W., Van Dyk, S. D., Panagia, N., Sramek, R. A., & Discenna, J. L. 1991, ApJ, 380, 161

This manuscript was prepared with the AAS LaTeX macros v4.0.

Parameters for Radio Observations

	1983-1984 Observations		1990-1992 Observations	
Wavelength (cm) :	20	6	20	6
Frequency (GHz) :	1.446	4.873	1.515	4.848
Bandwidth per IF (MHz) :	12.5	25	25	25
Number of IFs :	2	2	2	2
Observation dates :	15 Dec 1983	13 Mar 1984	4 Jan 1992	14 Oct 1990
Observing time (hr) :	6	6.5	8	8.5
VLA Configuration :	BnA	CnB	B	CnB
Primary beam HPBW :	$30'$	$8'$	$30'$	$8'$
Resolution ($\alpha \times \delta$) :	$3\farcs5 \times 3\farcs5$	$3\farcs9 \times 2\farcs8$	$2\farcs3 \times 5\farcs2$	$3\farcs2 \times 2\farcs8$
Rms noise (mJy beam^{-1}) :	0.19	0.054	0.050	0.028

Radio Observations

Source	R.A.(1950)[b]	Dec.(1950)[c]	Peak Flux (mJy) 20 cm	Peak Flux (mJy) 6 cm	Age (yrs)
SN 1923A?[a]	$13^h34^m19\overset{s}{.}92$	$-29°35'46\overset{''}{.}3$	< 0.57[d]	$\cdots$	60.6
			$\cdots$	0.19 ± 0.05	60.8
			$\cdots$	0.093 ± 0.03	67.4
			0.30 ± 0.05	$\cdots$	68.6
Eastern Source	$13^h34^m20\overset{s}{.}18$	$-29°35'46\overset{''}{.}6$	< 0.57[d]	$\cdots$	60.6
			$\cdots$	0.21 ± 0.05	60.8
			$\cdots$	0.13 ± 0.03	67.4
			0.29 ± 0.05	$\cdots$	68.6

[a] Optical position at $\alpha(1950) = 13^h34^m20^s \pm 0\overset{s}{.}02$, $\delta(1950) = -29°35'48'' \pm 0\overset{''}{.}24$ from Pennington, Talbot, & Dufour (1982).

[b] $\pm\, 0\overset{s}{.}18$

[c] $\pm\, 5\overset{''}{.}2$

[d] 3σ upper limit

Figure Captions:

Fig. 1.— (a) A 1.515 GHz (20 cm) contour map of approximately half of the field of view for M83 taken at the VLA in the B configuration on January 4, 1992. The beam size ($\alpha \times \delta$) is $2\farcs3 \times 5\farcs2$ and the rms noise level is 0.050 mJy beam^{-1}. The contour levels are at 0.17, 0.27, 0.60, 0.89, 1.19, 1.49, 1.79, 2.08, 2.38, 2.68, 2.98, 5.95, 8.93, 11.9, 14.9, 17.9, 20.8, 23.8, 26.8, 29.5 mJy beam^{-1}. SN 1957D (CRB) and SN 1923A are both visible in the map as well as several other sources from CRB including the radio bright central regions of M83. (b) A (20 cm) contour map of the region immediately surrounding the site of SN 1923A, magnified from the map in Figure 1a. Included in the map are both SN candidates visible near the center of the map in Figure 1a. A cross marks the optical position for SN 1923A from Pennington et al. (1982). The contour levels are -0.071, 0.071, 0.14, 0.17, 0.19, 0.21, 0.24, 0.26, 0.27, 0.29, 0.30 mJy beam^{-1}. The peak flux for the SN 1923A candidate is 0.30 ± 0.05 mJy beam^{-1}. (c) A (6cm) contour map of the region immediately surrounding the site of SN 1923A taken at the VLA in the CnB configuration on October 14, 1990. The beamsize ($\alpha \times \delta$) is $3\farcs5 \times 2\farcs8$ and the rms noise level is 0.028 mJy beam^{-1}. A cross marks the optical position for SN 1923A from Pennington et al. (1982). Both SN candidates are visible with peak flux positions consistent (to within uncertainties) with the 20 cm peak flux positions. The angular separation of the peaks of the two sources is nearly identical ($3\farcs5$) in the 6 cm map and in the 20 cm map. The contour levels are -0.065, 0.065, 0.076, 0.087, 0.098, 0.11, 0.12, 0.13 mJy beam^{-1}. The peak flux for the candidate nearest the optical SN position is 0.093 ± 0.03 mJy beam^{-1}.

Fig. 2.— Radio luminosity of SN 1923A compared to several extra-galactic intermediate-age supernovae and Galactic SNRs at 20 cm as a function of time since outburst. The peak flux densities for both sources are nearly equal, so we only plot a single data point as representative of the luminosity for SN 1923A. Data and fits (solid lines) for SN 1979C

from Weiler et al. (1986, 1991), SN 1980K from Weiler et al. (1986, 1992), SN 1983N from Weiler et al. (1986) and Cowan & Branch (1985), SN 1970G from Cowan et al. (1991), SN 1968D from Hyman et al. (1995) and SNe 1950B & 1957D from CRB. The dashed line is an extrapolation to the light curve of SN 1983N based on the Chevalier model.

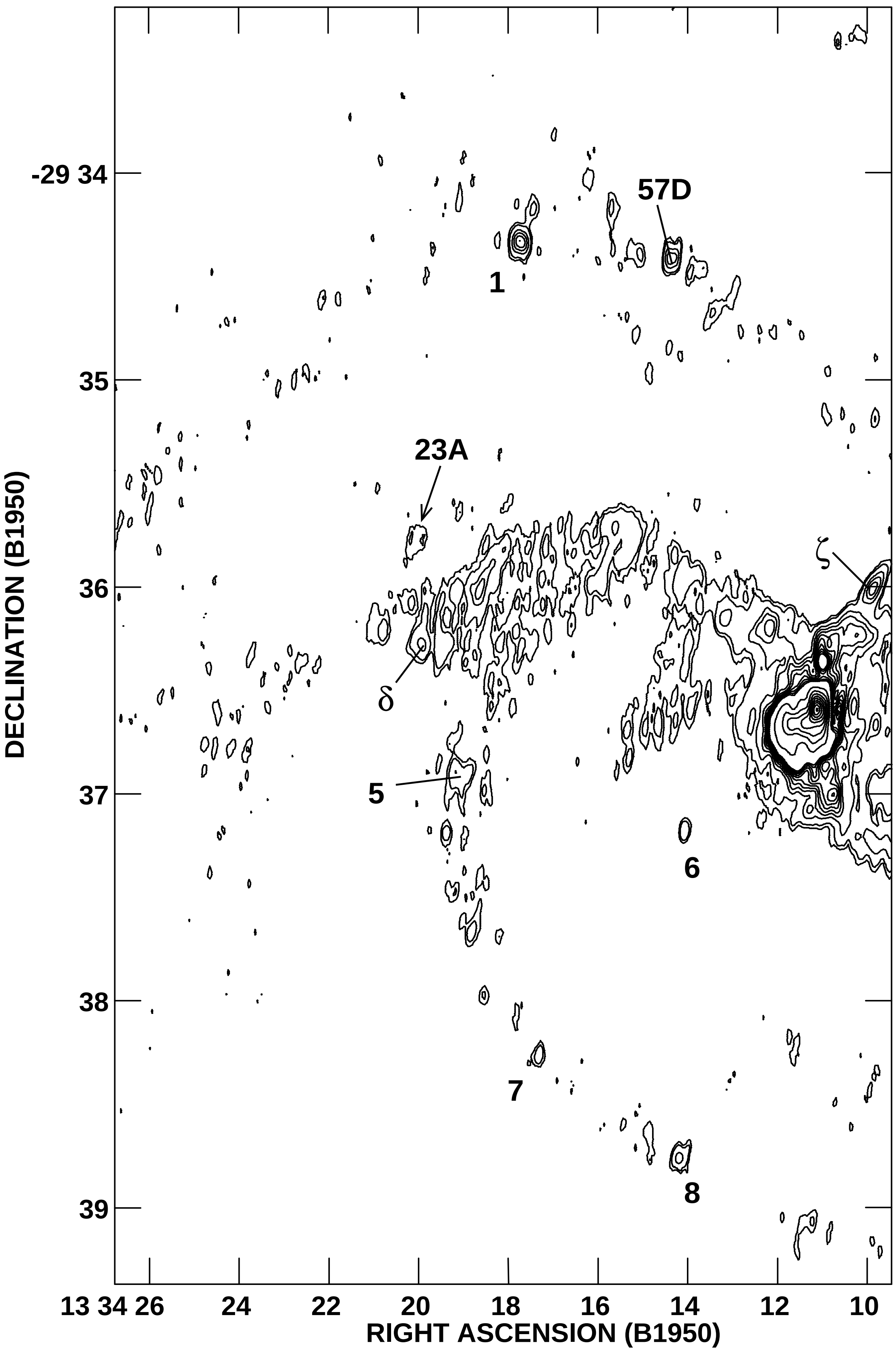
-29 34
35
36
37
38
39
DECLINATION (B1950)
13 34 26
24
22
20
18
16
14
12
10
RIGHT ASCENSION (B1950)
57D
1
23A
ζ
δ
5
6
7
8

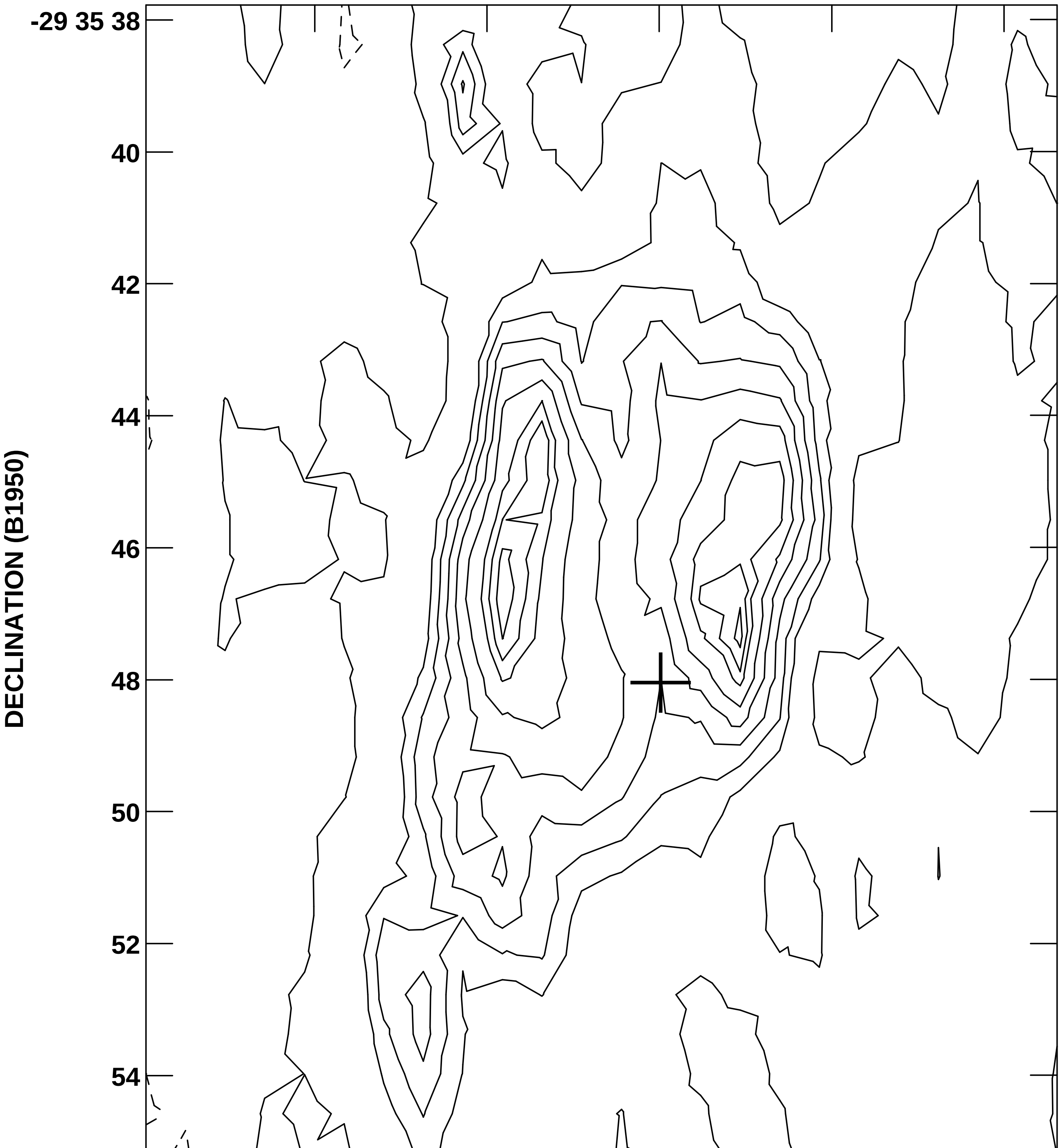

-29 35 38
40
42
44
46
48
50
52
54
56
DECLINATION (B1950)
13 34 20.4
20.2
20.0
19.8
19.6
RIGHT ASCENSION (B1950)

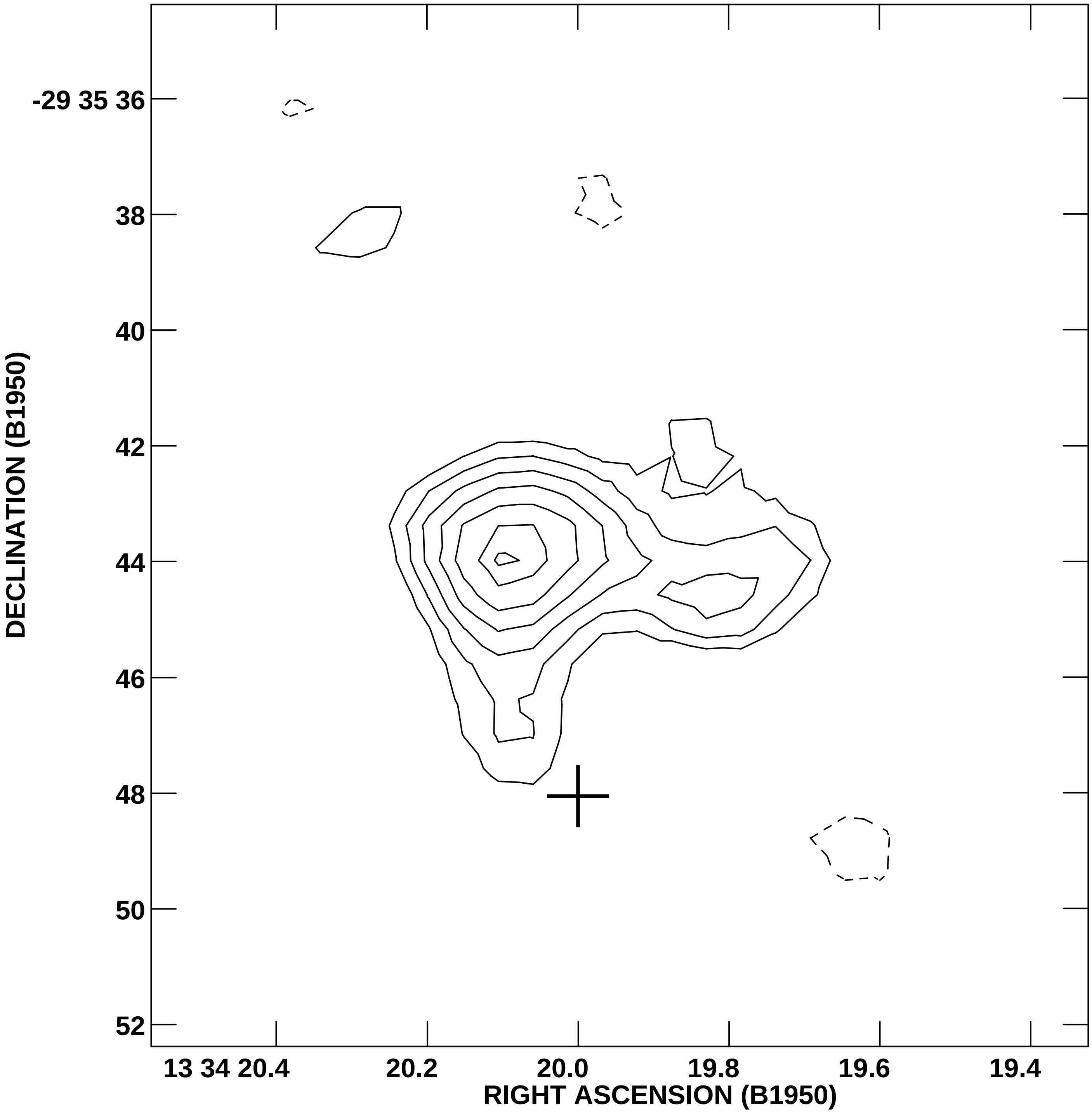

-29 35 36
38
40
42
44
46
48
50
52
DECLINATION (B1950)
13 34 20.4
20.2
20.0
19.8
19.6
19.4
RIGHT ASCENSION (B1950)

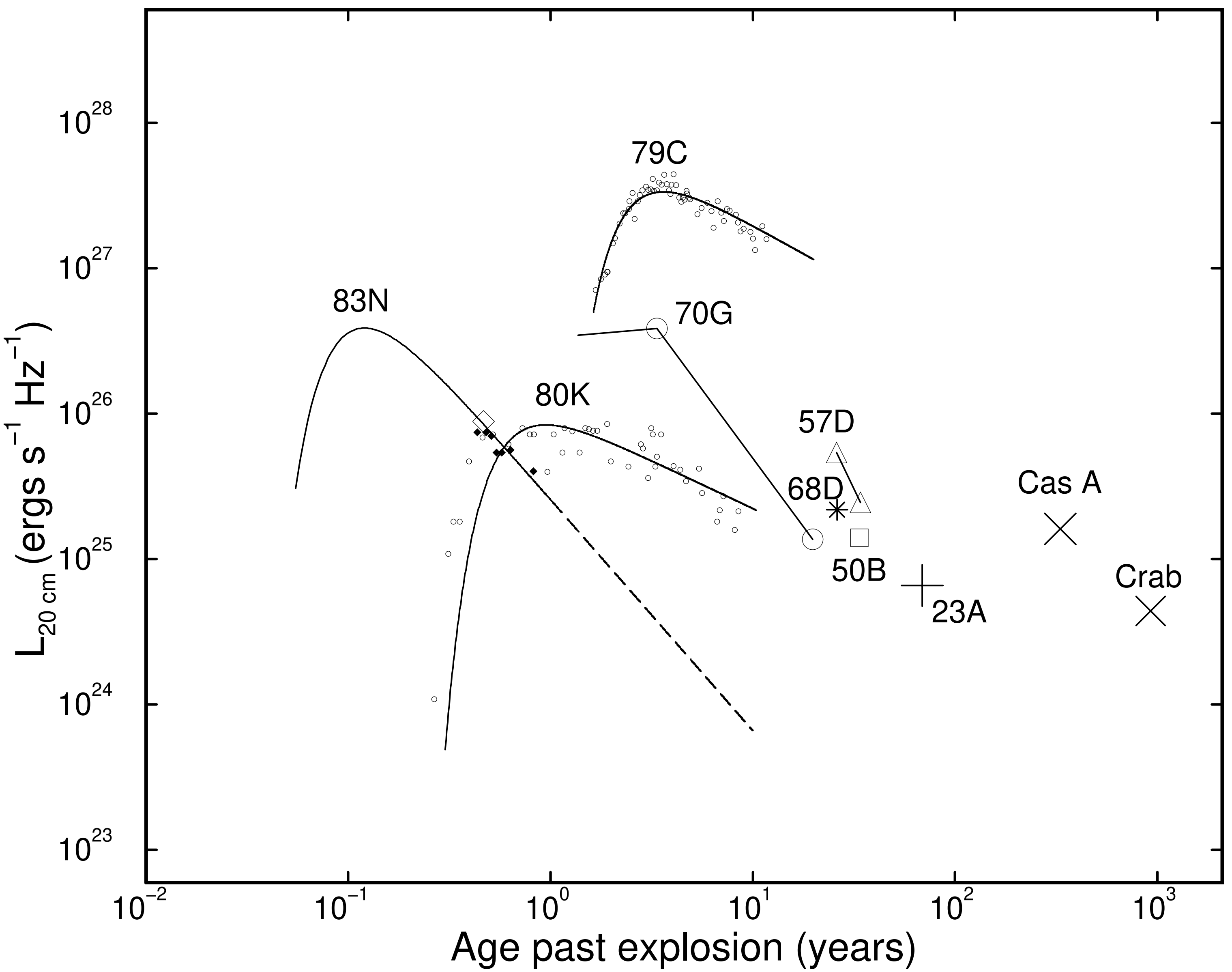

79C
83N
70G
80K
57D
68D
50B
23A
Cas A
Crab
10^{28}
10^{27}
10^{26}
10^{25}
10^{24}
10^{23}
$L_{20\ cm}$ (ergs s^{-1} Hz^{-1})
10^{-2}
10^{-1}
10^{0}
10^{1}
10^{2}
10^{3}
Age past explosion (years)